29 Mar 2001, 2:45 pm - 3:15 pm

Investigation of Seismic Soil-Footing Interaction by Large Scale Tests and Analytical Models

Ezio Faccioli
Politecnico di Milano, Italy

Roberto Paolucci
Politecnico di Milano, Italy

Guillermo Vivero
Universidad Politechnica de Madrid, Spain

INVESTIGATION OF SEISMIC SOIL-FOOTING INTERACTION BY LARGE SCALE CYCLIC TESTS AND ANALYTICAL MODELS

Ezio Faccioli
Dept. of Structural Engineering
Politecnico di Milano
Pza Leonardo da Vinci 32
20133 Milano, ITALY

Roberto Paolucci
Dept. of Structural Engineering
Politecnico di Milano
Pza Leonardo da Vinci 32
20133 Milano, ITALY

Guillermo Vivero
Dept. of Structural Mechanics
Universidad Politecnica de Madrid
Jose Gutierrez Abascal 2
28006 Madrid, SPAIN

ABSTRACT

Recent experimental and analytical research on seismic behavior of shallow foundations is illustrated. The most significant results on the seismic bearing capacity of footings with pseudo-static approaches are reviewed first, including an analytical formula recently proposed for the new version of the "seismic" Eurocode 8. Afterwards, we present the salient experimental results of large-scale cyclic tests of a shallow foundation model (1m x 1m in plan) resting on a large volume of sand, with relative densities 45% and 85%, discussing them in detail. Under earthquake-like cyclic loading, with peak values close to the pseudo-static failure limit, significant permanent settlement and rocking were observed, approaching serviceability limit states in low-density soil conditions. A series of displacement cycles of increasing amplitude was subsequently applied, up to the ultimate capacity of the soil-foundation system. Although the experimental cyclic bearing capacity is much higher than that predicted by pseudo-static approaches, this advantage is offset by the occurrence of large permanent deformations that may lead the structure to collapse. Finally, a recent theoretical method for performing simple nonlinear dynamic soil-structure interaction analyses is reviewed, and applied to estimating the reduction of response spectrum ordinates in strong earthquakes. Reductions up to 30%-50% were found for spectral accelerations exceeding 0.4g.

INTRODUCTION

This special presentation addresses some closely interconnected topics concerning the earthquake behaviour of shallow foundations.

The spectacular failures suffered by a number of recent buildings in Adapazari city, Turkey, during the disastrous Kocaeli earthquake of August 1999 provide outstanding field evidence on the role of rotations and overturning moments acting on shallow foundations during strong ground motion. These were mostly rigid body failures, sometimes with complete overtopping of the structure; affected buildings typically had a mat-type shallow foundation and rather large height/width ratio. Liquefaction .of foundation soils was certainly an important factor, but probably not the only one. Even in buildings that did not suffer spectacular failures and possibly rested on predominantly cohesive soils that prevented liquefaction, significant tilting and settlements were observed. According to Gazetas (2000), buildings in Adapazari with aspect ratio H/B < 1 did not experience visible tilting, even if they were free laterally; buildings with aspect ratio of about H/B ≈ 1.5 experienced tilting of about 5 degrees; and buildings with aspect ratio of H/B > 2 toppled, if of course they were free laterally.

One key question of interest for the geotechnical designer, discussed in the following sections, is the assessment of the "seismic" bearing capacity of foundations in the light of the most recent developments of this subject, including experimental validation by large scale tests. More specifically: how safe, in terms of permanent deformations, can we consider a foundation that satisfies a bearing capacity criterion where the design earthquake enters only in the form of pseudo-static actions? Does the fulfilment of the bearing capacity requirement impose excessive limitations on the foundation displacements and rotations, or vice-versa?

We give in the next section an outline of the most recent developments in the field of pseudo-static methods for bearing capacity assessment; based on such developments, the part of Eurocode 8 (1994) devoted to foundations and geotechnical aspects is currently being updated. Next, after reviewing recent experimental results, notably those obtained in the centrifuge, we illustrate perhaps the core of this presentation, namely the validation provided by large-scale cyclic test both to bearing capacity criteria and to methods for deformation analysis. These cyclic tests are of unprecedented size for the laboratory and the results have allowed to throw light on several significant aspects of the problem.

Finally, theory and experiments consistently indicate that both research and design applications would significantly benefit from improved accuracy in estimating permanent displacements resulting from nonlinear soil foundation interaction during strong earthquake shaking. A simplified method based on a macro-element approach is reviewed, and its application to determining the reduction of spectral response due to nonlinear dissipation of the soil foundation system is described.

PSEUDO-STATIC METHODS

The seismic bearing capacity of shallow foundations is generally checked using the classical superposition formula:

$$q_u = \tfrac{1}{2}\gamma S_\gamma i_\gamma N_\gamma + c\, S_c i_c N_c + q_y S_q i_q N_q \qquad (1)$$

where γ, c, q_y are the unit weight, soil cohesion and lateral overburden, respectively, and N_γ, N_c and N_q the well known bearing capacity factors, depending on the soil friction angle. The seismic action is treated as an equivalent static force that affects the S and i correction factors, taking into account the load eccentricity and inclination.

In the early 90s this approach has been improved by several theoretical studies based on limit equilibrium techniques (Sarma and Iossifelis, 1990; Budhu and Al-Karni, 1993; Richards *et al.*, 1993), where the effect of soil inertia on bearing capacity was included.

Although these studies contributed significantly to clarifying the subject, they suffered from the following main limitations:

- the effect of load eccentricity was not investigated, especially under high lateral loads that may induce foundation uplift;
- the effect of soil inertia was not separated from that of load inclination, leading to a partial misunderstanding of its consequences on bearing capacity.

These effects were thoroughly analyzed in subsequent papers (Pecker and Salençon, 1991; Dormieux and Pecker, 1995; Paolucci and Pecker, 1997a and b) using the upper bound (kinematic) approach of the yield design theory (Salençon, 1990).

Kinematic approach

The core of the kinematic approach is the assumption of one (or several) admissible kinematic mechanisms describing the velocity field of the soil-foundation system at failure. An example is shown in Fig. 1, in the case of a homogeneous cohesionless (Tresca) soil. This is an improvement on the classical Prandtl-type rupture mechanism, because foundation uplift is allowed. Any rupture mechanism is defined by a set Ψ of unknown geometric parameters (for example α, μ and λ in Fig. 1).

If we denote by Q the set of external loads applied to the foundation, by P^{ext} the power of such external loads, and by P^{res}, the maximum resisting power, depending on the soil strength and the mechanism geometry, the necessary condition of stability of the soil-foundation system requires:

$$P^{ext}(Q, \Psi) \le P^{res}(\Psi, \text{soil strength}). \qquad (2)$$

A minimization procedure applied to inequality (2) allows to find the upper bound of the external loads Q and the corresponding "optimum" parameter set of the rupture mechanism.

In the seismic case, the external loads typically include:

- vertical action (N)
- horizontal action (H)
- overturning moment (M)
- soil inertia force (F)

All admissible loads, satisfying (2), lie within the so-called *bounding surface* defined in the external load space as:

$$\Phi(N, H, M, F) \le 0. \qquad (3)$$

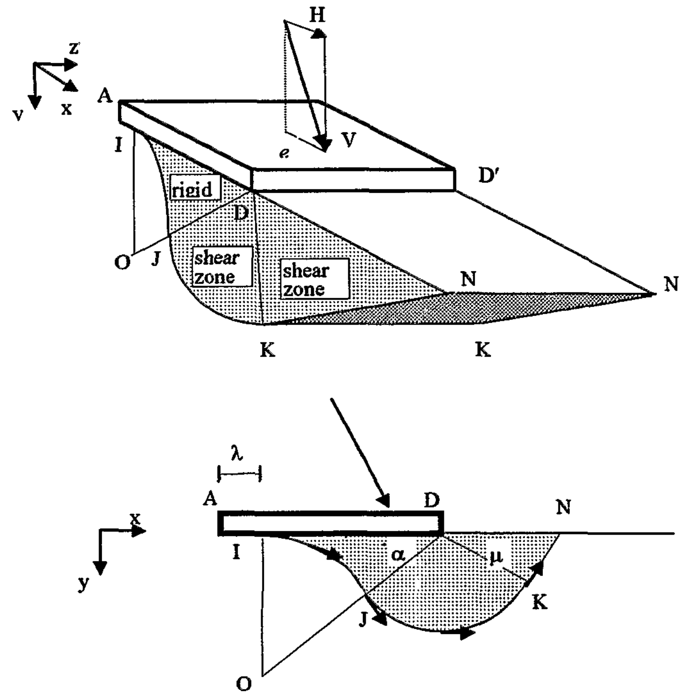

Fig. 1. 3D view of one of the kinematic mechanisms considered for bearing capacity calculations in cohesive (Tresca) soils. From Paolucci et al. (1997b).

Analytical formula for seismic bearing capacity calculations

Using the concept of bounding surface, as an alternative to the classical superposition formula (1), a new method has been introduced for computing the seismic bearing capacity of shallow foundations (Pecker, 1997).

Based on the results of a wide set of theoretical analyses using the kinematic approach, the following analytical expression of the bounding surface has been proposed for the new version of Eurocode 8 (Provisions for earthquake resistance of structures), presently under preparation:

$$\Phi(\overline{N},\overline{H},\overline{M},\overline{F}) = \frac{\left(1-e\overline{F}\right)^{c_T}\left(\beta\overline{H}\right)^{c_T}}{\left(\overline{N}\right)^a\left[\left(1-m\overline{F}^k\right)^{k'}-\overline{N}\right]^b} + \frac{\left(1-f\overline{F}\right)^{c'_M}\left(\gamma_M\overline{M}\right)^{c_M}}{\left(\overline{N}\right)^c\left[\left(1-m\overline{F}^k\right)^{k'}-\overline{N}\right]^d} - 1 \qquad (4)$$

where :

$$\overline{N}=\frac{\mu N}{N_{max}} \quad , \quad \overline{H}=\frac{\mu H}{N_{max}} \quad , \quad \overline{M}=\frac{\mu M}{B N_{max}}, \qquad (5)$$

N_{max} = ultimate bearing capacity under a vertical centered load, to be calculated by (1) with the appropriate material safety factor;

μ = partial safety factor that accounts for model uncertainty during dynamic loads, and depends on soil conditions as in Tab. 1;

B = foundation width;

$\overline{F}$ = dimensionless soil inertia forces defined as follows:

$$\overline{F}=\frac{\gamma k_H B}{c_u} \quad \text{for purely cohesive soil} \qquad (6a)$$

$$\overline{F}=\frac{k_H}{\tan\varphi} \quad \text{for purely cohesionless soil} \qquad (6b)$$

In the previous expressions, ϕ is the soil friction angle, c_u the undrained shear strength, and k_H the horizontal seismic design coefficient. The other parameters a, b, c, d, e, f, g, k, k', c_T, c_M, c'_M, β, γ_M are defined according to the soil nature, as given in Tab. 2.
The foundation is safe if, under the prescribed seismic loads, inequality (3) is satisfied.

A 3D elevation view of the bounding surface (4) in the case of cohesionless soils is illustrated in Fig. 2a, while two cross-sections are shown in Fig.2b, for the case $\overline{F}$=0 (no soil inertia) and eccentricity ratio e/B=0 and e/B=1/6. As discussed by Paolucci and Pecker (1997a) these curves are close to those obtained experimentally by other researchers (e.g. Nova and Montrasio, 1991; Butterfield and Gottardi, 1994). It can be easily verified from (4) that for $k_h < 0.1$ and reasonable values of the static safety factor, soil inertia effects can be neglected for cohesionless soils, while for cohesive soils $\overline{F}$ can be taken equal to 0.
Although the bounding surface (4) has a rather cumbersome expression, its use for seismic bearing capacity calculations presents several advantages:

- a single expression is used for purely cohesive and cohesionless soil conditions;
- it represents a theoretical upper bound for failure loads;
- the effect of soil inertia is accounted for explicitly.

Besides, if the soil inertia effect is neglected ($\overline{F}$=0), equation (4) takes a more "manageable" form.

LARGE-SCALE SOIL-STRUCTURE INTERACTION EXPERIMENTS

Overview of recent experimental results

Laboratory tests encounter several major difficulties for a sound experimental reproduction of the complex, nonlinear dynamic soil-structure interaction problem, such as:

- *careful control of soil properties*: the deposition procedure and the saturation (if required) of the soil specimen must be carefully conducted and checked;
- *boundary conditions*: the boundaries of the testing apparatus should be enough removed from the foundation so to prevent any constraint on the development of failure mechanisms. Besides, flexible boundaries should be used, with well calibrated properties to reproduce free-field boundary conditions;
- *scale problems*: large-scale tests are more expensive, involve a very large amount of material, and cannot be repeated easily, while the use of scaling laws in small-scale tests is questionable when applied to the grain size of soil materials, especially for strongly non-linear problems with pore-pressure build up;
- *seismic loads*: both seismic actions transmitted by the superstructure (vertical and shear force, plus overturning moment) and soil inertia effects should be taken into account simultaneously.

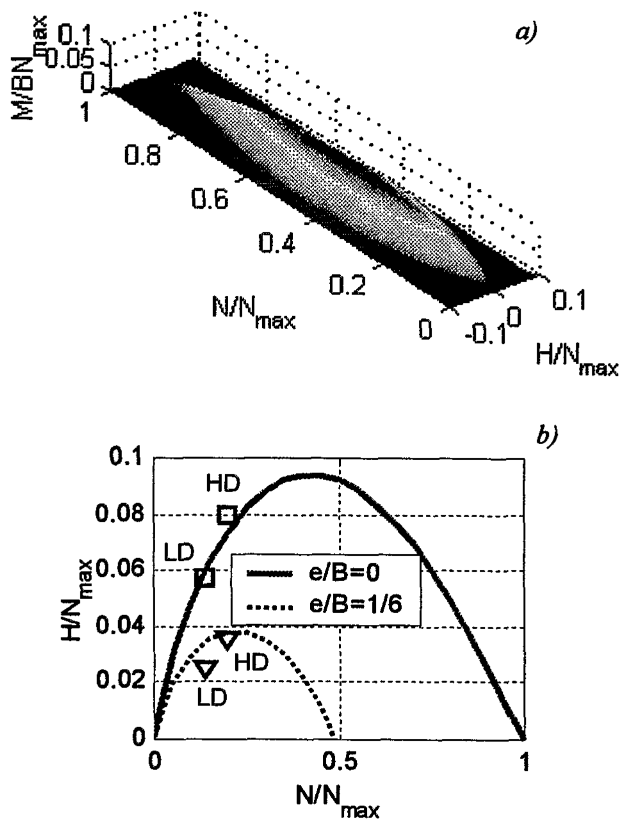

Fig. 2. a) 3D view of the bounding surface (4). b) Cross-sections of the bounding surface (4), in the case of no soil inertia and two different values of eccentricity ratio (e/B). Squares denote the limit value of the horizontal force H during Phase III of the large-scale cyclic tests, with e/B in the range 0.35-0.40. Triangles denote the peak value of H, during Phase II of the large-scale cyclic tests, with e/B=1/6.

Tab. 1. Partial safety factor μ to accounting for model uncertainties in seismic conditions (proposed for the new version of Eurocode 8, under preparation).

Medium-dense to dense sand	Loose dry sand	Loose saturated sand	Non sensitive clay	Sensitive clay
1.0	1.15	1.50	1.0	1.15

Tab. 2. Parameters in the equation (4) of the bounding surface.

Parameter	Purely cohesive soil	Purely cohesionless soil
a	0.70	0.92
b	1.29	1.25
c	2.14	0.92
d	1.81	1.25
e	0.21	0.41
f	0.44	0.32
m	0.21	0.96
k	1.22	1.00
k'	1.00	0.39
c_T	2.00	1.14
c_M	2.00	1.01
c'_M	1.00	1.01
β	2.57	2.90
γ_M	1.85	2.80

It is impossible to cope with all of these requirements with the same testing apparatus. Centrifuge testing has encountered a notable success in the recent years, with several applications to the seismic analysis of shallow foundations (see e.g. Zeng and Steedman, 1998; Garnier and Pecker, 1999). Another potentially useful apparatus for testing geotechnical structures is the shear stack mounted on the shaking table of the University of Bristol (Taylor *et al.*, 1994), that allows to perform large-scale experiments and to closely simulate free-field boundary conditions.
Zeng and Steedman carried out a series of centrifuge experiments with medium-dense (relative density varying in the range 46-63%) and dry or saturated soil conditions. A summary of test results is given in Tab. 3. In the most favourable conditions, consisting of a light foundation model with high static safety factor and low aspect ratio (height of the center of gravity/foundation width) the foundation underwent only slight permanent deformations even under several peaks of horizontal acceleration of 0.45g.
In a subsequent series of tests with a "heavy" model (static safety factor about 8, with aspect ratio 1.5), the foundation failed both on dry and saturated soil, under cycles of peak ground acceleration ranging between 0.24g and 0.31g.
The key parameter leading foundation to failure was identified by the authors as the foundation rotation cumulated during several cycles of loading, leading to a progressive reduction of the contact area between soil and foundation.

Large-scale experimental setup

A programme of large-size, cyclic loading experiments has been carried out in 1997-98, by the first two authors and other specialists, within the framework of the European research Project TRISEE (3D Site Effects and Soil-Foundation Interaction in Earthquake and Vibration Risk Evaluation, see Internet site http://www.crs4.it/trisee), to investigate the non-linear interaction between direct foundations and the supporting soil under seismic loading. The basic set-up of the experiments consists of a footing lying on a saturated sand of known properties, and excited by a time-varying horizontal force and moment, intended to simulate the inertial forces transmitted to the foundation by the superstructure. The soil mass is at rest, so that the wave propagation and inertia effects in the soil are neglected with respect to the dynamic inertia forces transmitted by the foundation. As mentioned in the previous section, soil inertia has a negligible influence on the failure loads for reasonable values of the static safety factor.
The tests were performed at the soil relative densities $D_r \approx$ 85% and $D_r \approx$ 45%, that are representative of high (HD) and low density (LD) soil conditions. The latter can be considered as a lower bound for design of shallow foundations in practice, since the presence of sands at lower density generally leads the engineer to other design solutions.
The experimental prototype consists of a stiff concrete caisson filled with sand (Ticino sand, described in Bellotti *et al.*, 1996), and of a steel mock-up, representative of a concrete footing, see Fig. 3. The caisson has dimensions 4.60 m by 4.60 m in plan and 4 m in height, while the foundation is 1 m by 1 m in plan. The walls of the caisson are rigid and waterproof. While the bottom of the caisson is enough removed from the foundation to avoid interference with the possible failure mechanisms, the vertical walls may have a significant influence on the bearing capacity of the foundation on dense sand, that should be taken into account in the interpretation of experimental results. On the other hand, the effect of the lateral constraints on the development of permanent displacements and rotations is less important, except at failure.
The foundation is made of steel, and has a concrete interface with the underlying soil that ensures a high friction resistance under horizontal loads. As shown in Fig. 1, the foundation is embedded 1 m in the sand, corresponding to a lateral overburden of about 20 kPa. A 1 m high steel formwork was placed around the foundation to retain the sand.
The vertical load is transmitted by an air cushion system designed to keep the force constant throughout the test. A hydraulic actuator, acting 0.9 m above the foundation level, transmits to the foundation the prescribed time-varying horizontal force or displacement.
Details on the reconstitution and saturation of the soil samples, on the evaluation of soil properties and on the instrumentation are reported elsewhere (Jamiolkowski *et al.*, 1999). Full saturation of the soil mass was attempted but could not be attained, so that the tests should actually be representative of drained soil conditions.

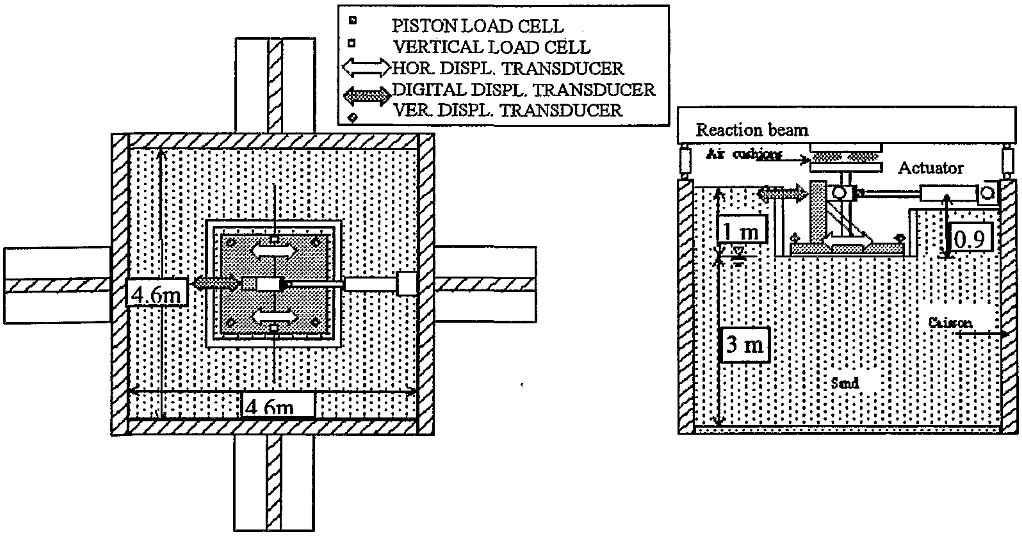

Fig. 3: Scheme of the experimental setup.

Tab. 3. Summary of experimental results on shallow foundations under seismic loads, from centrifuge tests and large-scale tests.

	Static safety factor	Aspect ratio	Relative density	Soil conditions	PGA (g)	Peak Rocking (mrad)	Peak Settl. (mm)	Residual Rocking (mrad)	Residual Settl. (mm)
Centrifuge tests (Zeng and Steedman, 1998)									
C1	60	0.5	52	dry	0.45		20	0	20
C2	60	0.5	57	satur.	0.19	3.5	4	0	4
C3	8	1.5	55	dry	0.31	failure due to progressive rotation			
C4	4	1.5	63	satur.	0.24	failure due to progressive rotation			
Large-scale tests									
LS1	7	0.9	45	satur.	0.18	6	11	2	11
LS2	5	0.9	85	satur.	0.18	3	3	0.5	3

Test sequence

The HD and LD specimens were subjected to a similar test sequence, consisting of the application of the design-level vertical load (which was kept constant throughout the whole loading sequence), and of three subsequent cyclic loading phases reproducing different levels of horizontal excitation. The design vertical loads were 300 kN and 100 kN for HD and LD specimens, corresponding to design pressures of 300 kPa and 100 kPa, respectively. These are typical design values for foundations on medium to dense sands, and are governed by admissible settlement requirements. The resulting static safety factor, based on the superposition formula (1), was found to be about 5 in HD and 7 in LD conditions.
The final vertical settlement experienced by the foundation under static load was about 7 mm for HD, and about 16 mm for the LD soil conditions. A detailed analysis of the static settlements can be found elsewhere (Jamiolkowski *et al.*, 1999).
After completion of the static loading, the horizontal cyclic loading was applied in three phases, as follows.

Phase I. A series of small-amplitude, force-controlled pulses was applied first, to identify the onset of non-linear behaviour in the soil. Each pulse consisted of two sinusoidal cycles, with frequency f=0.5 Hz. Their amplitude was gradually increased up to about 5% of the vertical load, to obtain evidence of stiffness degradation and development of hysteresis loops.

Phase II. The foundation was then subjected to an earthquake-like variable horizontal force and overturning moment transmitted by the hydraulic actuator at 0.9 m height. The time history of the horizontal force was adapted from that of the base-shear measured on a four-story RC building, designed according to EC8 and tested at the ELSA laboratory (Negro *et al.*, 1996). The peak of the seismic excitation was scaled to a seismic coefficient (horizontal force divided by vertical force) of about 0.2, as shown in Fig. 4. The seismic coefficient was combined with the height of application of the horizontal force (h=0.9m) in such a way that a compressive stress was maintained everywhere on the foundation interface. The absolute value of the force peak was of about 60 kN and 20 kN for the HD and LD tests, respectively. To preserve the accuracy in the force-control system, the original time scale was expanded. For the HD test, the time scale was expanded by a factor of 6, whereas for the LD test the original time scale was expanded by a factor of 3. Since the original record of horizontal force had a fundamental frequency of about 0.8 Hz, the horizontal force diagram actually applied had, instead, a fundamental frequency of 0.13 Hz for the HD test and of 0.27 and for the LD test.

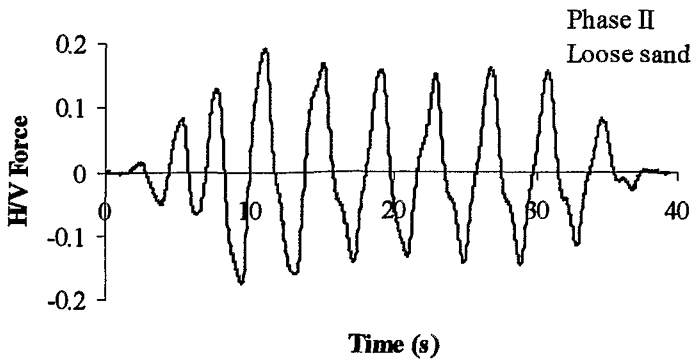

Fig. 4: Phase II: time-history of normalized horizontal force

Phase III. Finally, sine-shaped displacement pulses of increasing amplitude were imposed to the top of the structure, up to the attainment of a limit threshold of the foundation resistance. In this final phase, the test was displacement-controlled in order to avoid excessive movement of the system close to its ultimate capacity. Pairs of cycles (f=1/6 Hz) were used for HD test and single cycles (f=1/3 Hz) for LD test.

Main test results

Phase I The application of force-controlled cycles of small amplitude resulted in substantially similar behaviour in the two tests. The hysteresis loops for the overturning moment vs. rocking were narrow and quite stable, denoting a limited amount of dissipation. The rocking stiffness for the HD case was more than twice that in the LD case. The settlement of the foundation at the end of this phase was about 0.15 mm in both HD and LD cases, indicating that for values of the seismic coefficient not exceeding about 0.05 g, the permanent foundation displacement and rocking are negligible.

Phase II. This loading phase is the most meaningful for throwing light on foundation behaviour under earthquake loading. Representative results are illustrated in Figures 5 and 6, namely the overturning moment vs. rocking diagrams and the vertical settlements, respectively. In both HD and LD tests, the largest cycle occurred for the peak of horizontal force, while the subsequent cycles were essentially contained inside this loop. During the most severe cycle, stiffness reduced to about 30% of the initial value for the HD case, and to about 20% for the LD case. However, as shown in Fig. 5, the initial stiffness is gradually recovered in the subsequent cycles.

Note that in this phase the seismic coefficient does not exceed 0.2 and the peak eccentricity ratio is e/B=1/6. In such conditions, the seismic loads lie on, or very close to the failure surface (4), as shown by the triangles in Fig. 2. However, the permanent deformations of the foundation were significant, especially in terms of rocking (see Tab. 3). Recalling that a foundation rotation of 2 mrad is considered as a threshold value for the onset of cracking on the superstructure (e.g. Lambe and Whitman, 1969), this value is slightly exceeded during several cycles in the HD case, while in the LD case the peak rocking reaches 6 mrad. The latter value is the relative rotation likely to cause an ultimate limit state in static conditions (Lambe and Whitman, *cit.*). At the end of this phase, the permanent rotation in the LD test was about 2 mrad. Vertical settlements experienced by the foundation are less severe than rocking, in terms of serviceability limit state. However, for LD conditions, the final settlement was about 10 mm, or 60% of the static vertical settlement. For HD conditions, the settlement increment is about 30%.

These results point to the need of improving the accuracy of current predictions of foundation settlements and rocking caused by earthquakes; the indication is that the movements may attain significant values, possibly beyond serviceability limit states, even under a moderate seismic excitation like that considered in these tests.

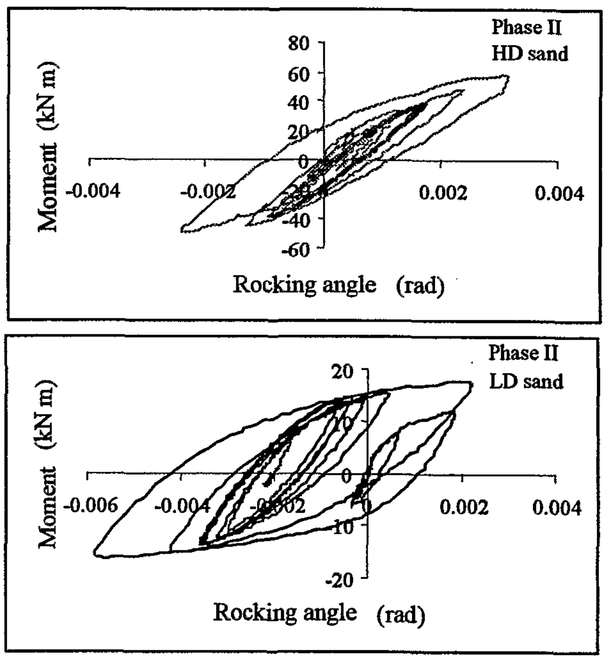

Fig. 5: Phase II: Overturning moment vs. rocking for HD and LD conditions.

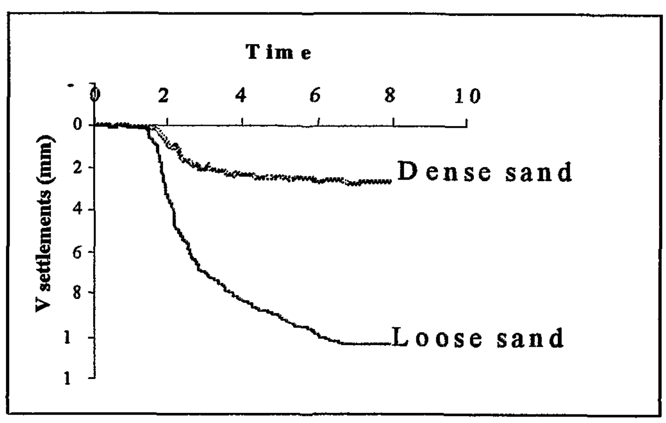

Fig. 6: Phase II: Vertical displacement of the foundation.

Phase III. During this phase, displacement-controlled cycles of increasing amplitude were applied to the foundation with the aim of reaching the ultimate foundation resistance.

The loops described by the curves of overturning moment vs. rocking are remarkably regular (Fig. 7). For the HD case, not shown in Fig. 7, the loops exhibit a characteristic S-shape, which has been satisfactorily modelled and interpreted in terms of foundation uplift under eccentric loading (Pedretti, 1998). This effect does not appear for LD conditions, since "punching" is the prevailing failure mode of the foundation in low to medium dense conditions (Vesic, 1973): the foundation sinks into the sand and uplift effects are prevented.

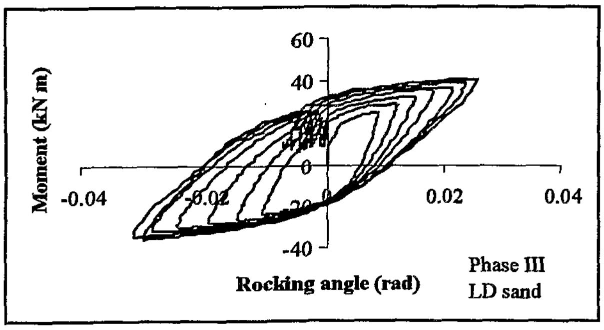

Fig. 7: Phase III: Overturning moment vs. rocking for LD conditions.

As a consequence of foundation punching, in the LD test settlements were observed to increase linearly in this phase, probably due to the progressive expulsion of sand from underneath the plate toward the sides during the sinking of the foundation. A linear increase of settlements occurred also for HD conditions, but final values in this case did not exceed 20 mm.

In Fig. 8 foundation settlements are plotted as a function of the seismic coefficient k_h. A limit value of k_h slightly lower than 0.4 is suggested by the curves, both for HD and LD soil conditions. However, such value cannot be straightforwardly interpreted to correspond to attainment of the true bearing capacity limit, even in the HD case. First, the lateral walls of the concrete caisson are too close to the foundation for a shear failure mechanism to completely develop, so that the observed bearing capacity should increase with respect to the theoretical value. Second, the experiments were carried out in cyclic loading conditions, that generally lead to an increase of the bearing capacity with respect to the conventional monotonic loading (Vesic, 1973). Considering again Fig. 2, the experimental values of H/N_{max} corresponding to cyclic failure are denoted by squares and compared with the pseudo-static limit curves. Recalling that at failure a peak load eccentricity e/B = 0.35 was attained, the experimental values are much higher than those corresponding to such eccentricity, and tend to lie on the curve corresponding e/B=0.

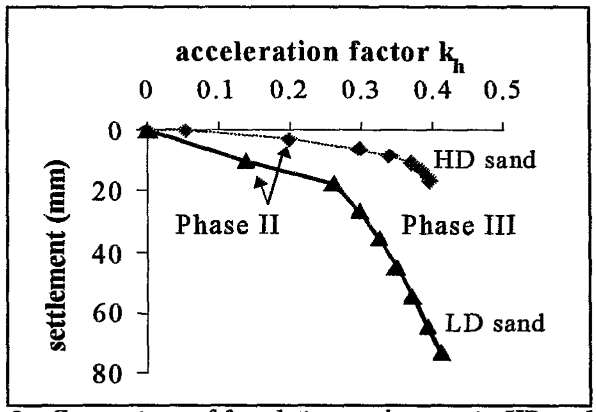

Fig. 8 - Comparison of foundation settlements in HD and LD soil conditions as a function of the seismic coefficient (k_h=H_{max}/N). From Pedretti (1998).

For application to soil-foundation interaction analyses with linear equivalent stiffness and damping, we have estimated from the experimental force-displacement cycles of loading phase III, shown in Fig. 9, the values of some such parameters. With reference to Fig. 10, a secant stiffness K was measured by the slope of the line joining the extreme points of the force – displacement cycle, while the damping factor η was obtained from the area D of the hysteresis loop(dissipated energy) and the stored elastic energy ΔW through the standard expression

$$\eta = \frac{D}{4\pi\Delta W} \qquad (7).$$

The low-strain horizontal stiffness K^0_H was computed from the nearly constant slope of the narrow loops observed in loading phase I; its HD value was 110 MN/m. The stiffness and damping estimates for the soil-foundation system were limited to the case of horizontal force and displacement in the HD test, because the phase III cycles in the LD test were severely non-symmetric due to the occurrence of large permanent horizontal displacement and rotations. On the other hand, as previously mentioned, the phase III moment–rotation cycles in the HD test were affected by partial foundation uplift, and because of this the associated values of the equivalent parameters are not discussed here.

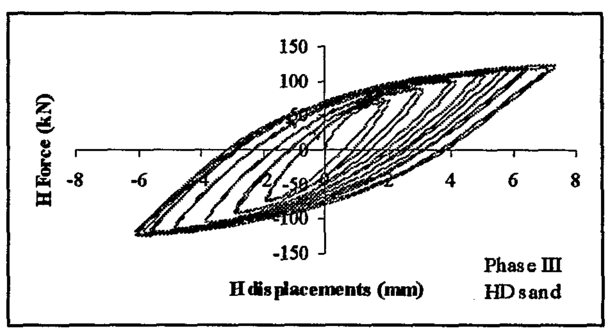

Fig. 9: Phase III: Horizontal force vs. displacement for HD conditions.

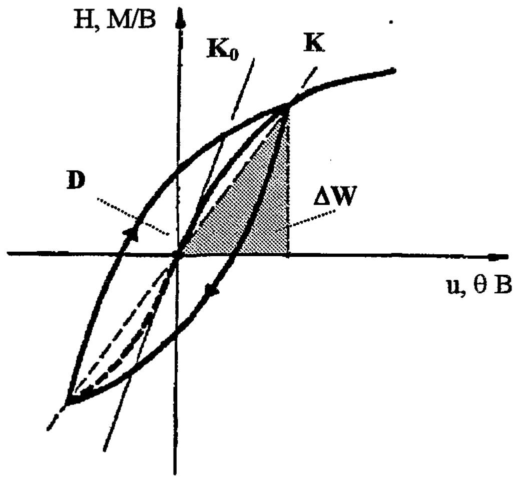

Fig. 10. Typical non-linear stress-strain curve under cyclic loading.

Figure 11 illustrates, on the left, the normalized translational stiffness K_H/K^0_H as a function of the peak horizontal foundation displacement observed in each cycle. On the horizontal axis, we also show a characteristic value γ_c of the shear strain in the soil, which was estimated by simply dividing the horizontal displacement by the width of the foundation (1 m). Similarly, the graph Fig. 12 displays the equivalent damping η vs. the same previous variables on the horizontal axis. The decay trend of the normalized stiffness in Fig. 11 appears generally consistent with the experimental shear modulus (G/G_{max}) vs. cyclic shear strain curves, albeit the values are on the high side. On the other hand, the η values fall within the range of experimentally observed values, as shown in Fig. 12. It should, be noted however, that the experimental curves of soil shear modulus and damping as a function of cyclic shear strain are ill defined in the large strain range involved in the present tests.

DYNAMIC METHODS

Truly dynamic approaches to the evaluation of permanent foundation displacements during earthquakes have been relatively few, and mostly limited to the well-known method of Newmark (1965), under the basic assumption that such displacements develop only after a critical load has been reached, typically the failure load, and that the superstructure and foundation response are decoupled. Examples of application of such approach to the seismic behaviour of shallow foundations can be found in Sarma and Iossifelis (1990), Richards *et al.* (1993), Pecker and Salençon (1991). One of the main drawbacks of the Newmark approach is that nonlinear interaction effects between the foundation and the superstructure are neglected. This may lead typically to the overestimation of the seismic actions transmitted by the superstructure and the inaccurate evaluation of the fundamental frequency of the interacting system.
On the other side, the rigorous modelling of the soil-foundation-superstructure system by dynamic finite-element analyses can be prohibitive in terms of computational effort, owing to the transient nature of the problem and the need for an accurate mathematical description of soil behaviour (Faccioli and Paolucci, 1996).

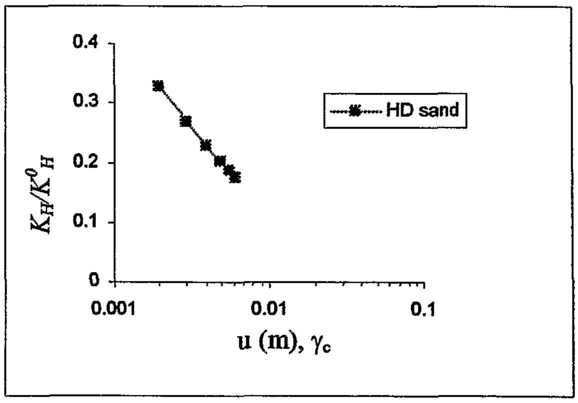

Fig. 11. Decay of the translational stiffness K_H, estimated from the hysteresis loops in Fig. 9. From Pedretti (1998)

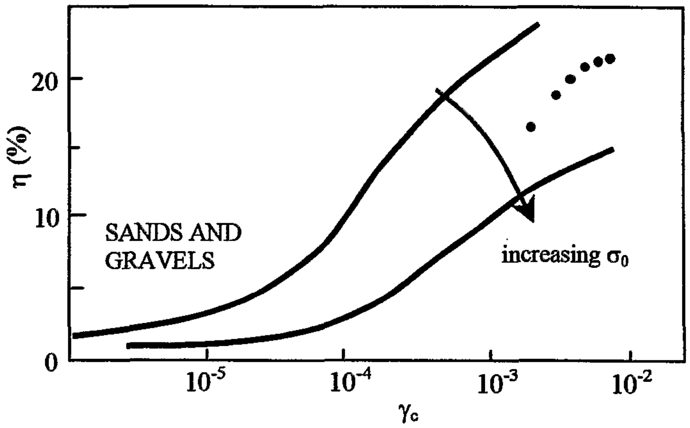

Fig. 12. Increase of damping ratio with shear strain amplitude. Dots indicate values estimated from results of large-scale tests on shallow foundations, as explained in the text. Modified after Seed et al., 1986.

The macro-element approach

An alternative promising method for capturing the salient features of the coupling between the nonlinear response of the soil-foundation system and the superstructure, and reasonably predicting the development and magnitude of permanent displacements, is the *macro-element* approach. Originally introduced by Nova and Montrasio (1991) for the theoretical analysis of shallow foundations under static loading, it has been first applied to the seismic case by Paolucci (1997).
The crucial idea behind this approach is to concentrate the material or geometrical (uplift) nonlinearities occurring at the soil-foundation interface in a single element described by an adequate elasto-plastic constitutive law.
Paolucci (*cit.*) modelled the dynamic nonlinear soil-structure interaction problem by a 4 degrees of freedom (DOF) system (Fig. 13), with the following basic assumptions:

- 1 DOF for the structure (horizontal translation) and 3 DOF for the foundation (horizontal and vertical translation, rocking);
- nonlinearity concentrated in the foundation DOFs;
- elastic behaviour of the foundation until the yield surface is reached.
- spring and dashpot coefficients to model soil-structure interaction (SSI) in the elastic range, calculated by standard formulas (e.g. Gazetas, 1991).
- perfectly plastic flow (no hardening), with non-associated flow rule.
-

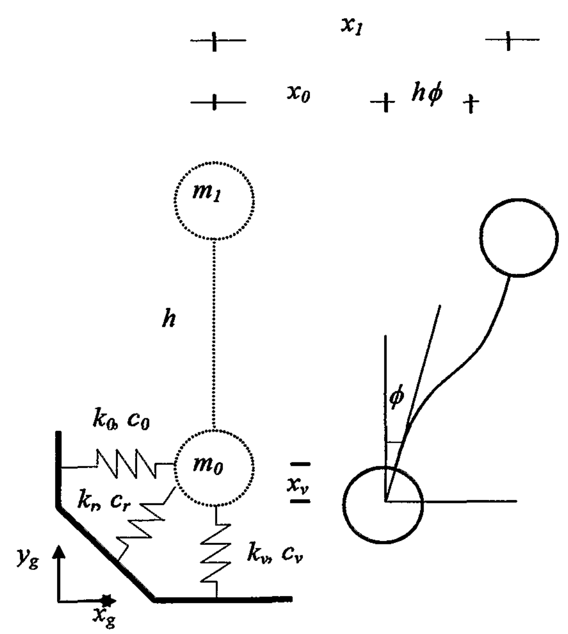

Fig. 13. Four degrees of freedom model for nonlinear dynamic soil-structure interaction analyses. From Paolucci (1997).

More recently, these assumptions have been refined to take into account foundation uplift by Cremer *et al.* (1999) and more complex constitutive descriptions of soil behaviour by Pedretti (1998) and Le Pape *et al.* (1999).
It must be stressed that, while numerous analytical or experimental works exist for the definition of a yield surface for shallow foundations, e.g. the bounding surface defined by (4), there are few experimental data to support the choice of a plastic potential function. Recent studies (Gottardi et al., 1999; Le Pape et al., 1999) may be helpful to fill this gap.

Reduction of spectral ordinates due to soil nonlinearity

While the evaluation of permanent deformations of shallow foundations during earthquakes has been thoroughly dealt with by Paolucci (1997), we analyse here the effect of soil yielding on the base shear transmitted by the superstructure.
For this purpose we have selected three real configurations, consisting of bridge piers on shallow foundations (Vivero, 2000). Foundations widths vary in the range from 5 to 9 m with 1-2 m of embedment. Medium-dense soil conditions at foundation level were considered, with a representative value of shear wave velocity Vs=200 m/s to calculate the spring and dashpot coefficients of the SSI problem. The fixed-base fundamental period of the systems under study varies between 0.5 s and 1 s, while the elastic soil-structure interaction was found to induce a moderate increase of the fundamental period, ranging from 8% to 12%.
Starting form these configurations, we made some slight realistic changes to structural properties, especially in terms of pier height and structural mass, and generated a set of "fictitious" structures that allowed to cover in a dense way the period range from 0.4 and 1.2 s.
Each fictitious structure, modelled by the nonlinear oscillator of Fig. 13, was shaken by several real accelerograms, representative of various levels of ground motion severity. We illustrate here the results in terms of spectral accelerations (Fig. 14) and spectral displacements (Fig. 15), respectively, only for the most severe accelerograms. The nonlinear effects induced by the ground motions of smaller amplitude were negligible.
In Figs. 14 and 15 the continuous line is the elastic response spectrum, while the three dotted lines represent the computed peak response of the nonlinear oscillator, starting from the three different real configurations discussed previously.
Some interesting comments on these results are in order:

- The reduction of base shear due to nonlinear SSI effects is negligible for spectral accelerations less than about 0.4 g. The same indication was derived by Paolucci (1997) in terms of permanent deformations of foundation soil.
- The nonlinear acceleration spectrum is smoothed with respect to the linear one, with peak reduction factors between about 30% and 50 % for the highest spectral ordinates.
- The nonlinear effect is to smooth the isolated peaks in the elastic displacement spectrum, but the average reduction is considerably lower than in the acceleration spectrum.
- The considerable "beneficial" effect on the superstructure is offset by permanent settlement and/or rocking at foundation level. Paolucci (1997) found that if the elastic spectral acceleration exceeds 0.4 g (Fig. 16), permanent damage to the foundation system may increase rapidly and reach values beyond the serviceability limits.

These results support both the need for improving the analytical tools for predicting footing displacements under dynamic loads, and the search for innovative design approaches capable of "controlling" the nonlinear behaviour of the soil-foundation system under strong loading. An example of such innovative approaches is the "capacity design" philosophy applied to the foundations of the Rion Antirion bridge near Patras, Greece (Pecker, 1998). In this case, the careful control of material grading and reinforcement was used as an effective method to constrain the foundation to dissipate energy in the sliding mode rather than in the overturning mode, that would be more harmful for the overall behaviour, especially for tall structures.

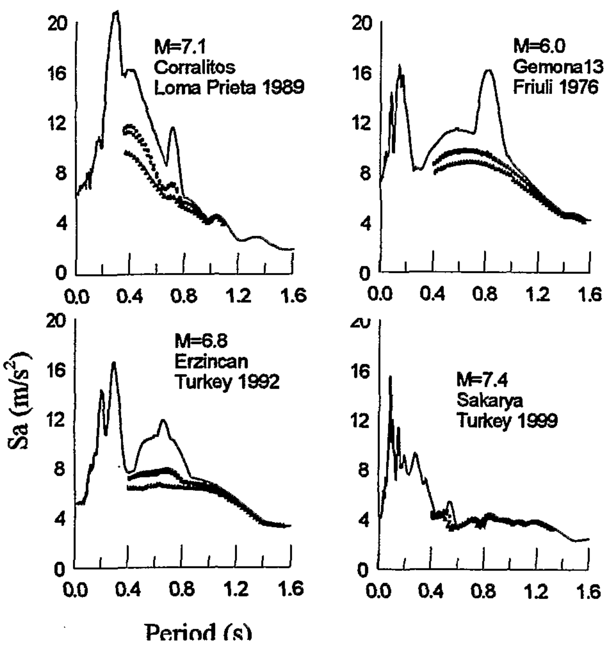

Fig. 14. Acceleration response spectra for different base accelerograms. Continuous line: elastic spectrum. Dotted lines: peak response of the nonlinear oscillator of Fig. 13, starting from three different real configurations.

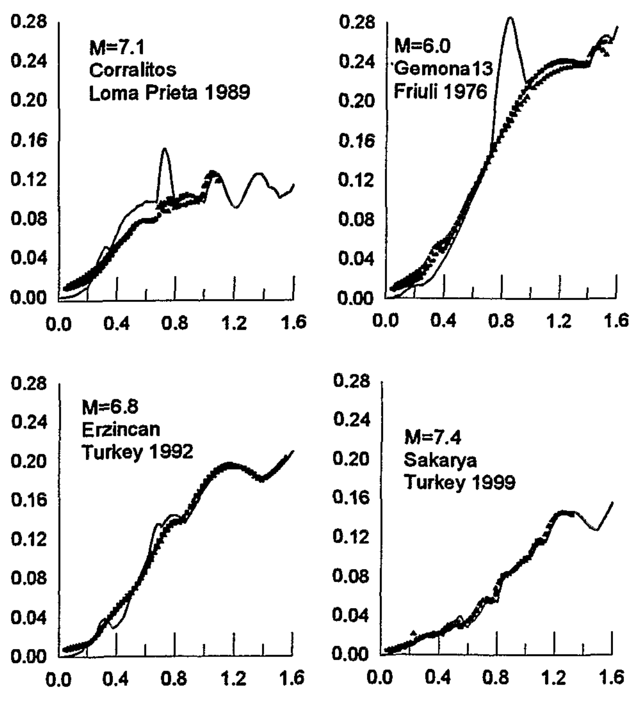

Fig. 15. As in Fig. 14, but for displacement response spectra.

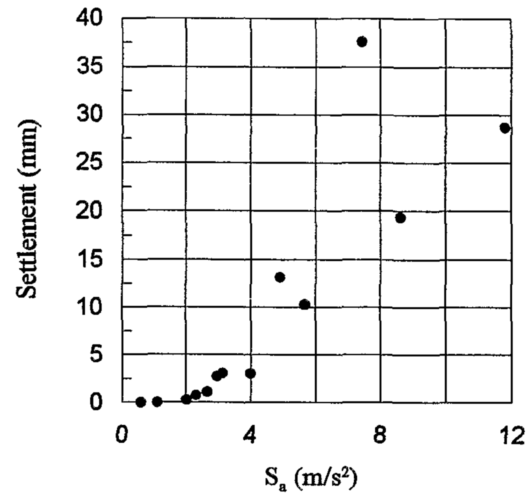

Fig. 16. Permanent settlements as a function of the response spectral ordinate, calculated with the simple oscillator of Fig. 13, with fundamental fixed-base period T=1s, subjected to real accelerograms with different levels of severity. Adapted from Paolucci (1997).

CONCLUSIONS

We have illustrated some recent relevant research developments on the seismic behaviour of shallow foundations. Emphasis has been given to analytical methods, such as pseudo-static and simplified dynamic approaches, and to the experimental results from well-calibrated and accurate large-scale tests on soil-footing interaction under cyclic loading. We summarize here some of the most relevant conclusions of our work.

- Large-scale cyclic tests represent a valid experimental approach for the analysis of soil-structure interaction effects during seismic loading. Their main advantages are the following: a) full-scale modelling; b) accurate determination of soil properties; c) application of realistic time histories of horizontal force and overturning moment. On the other side: a) soil inertia forces are not taken into account, b) lateral and bottom boundaries are close to the foundation and cannot reproduce completely free-field conditions, c) repetition of the experiment involves the treatment of a large amount of soil material.
- During the moderate excitation used in the earthquake-like loading phase of the cyclic tests, (seismic coefficient k_h=0.18), the seismic loads were very close to the pseudo-static failure surface, but did not exceed it. Even in such "safe" conditions, permanent settlements and rocking in the LD test attained values (see Tab. 3) that may affect significantly the serviceability of the structure. In the HD test permanent deformations were below a serviceability limit state, but nevertheless significant.
- The bearing capacity in cyclic loading conditions is much higher than obtained by pseudo-static approaches. However, this is offset by the development of permanent deformations well beyond the ultimate limit state for the structural safety.
- Based on the previous results, the use of a pseudo-static failure surface to delimit safe seismic loading conditions,

such as defined in equation (4), seems a sound approach to the seismic design of shallow foundations. Care should be taken in LD conditions, because final settlements and rocking may attain considerable values.

- This points to the need of improving our capabilities of prediction of earthquake-induced settlements: the macro-element approach, described in this paper, seems to be one of the most promising tools for simple estimates in dynamic conditions.
- Using the macro-element approach, we have found that under strong earthquake loading, indicatively with response spectral ordinates exceeding 0.4 g, the base shear reduction may attain values ranging from 30% to 50%. If the non-linear effects at the foundation level are controlled adequately, this may be an effective method for reducing seismic actions on the superstructure.

ACKNOWLEDGMENTS

The authors are grateful to Prof. A. Pecker for fruitful suggestions on the manuscript and to Dr. S. Pedretti, for making some figures available. Large-scale experiments were partially funded by the EC contract n. ENV4-CT96-0254 (TRISEE), while the studies on the reduction of spectral ordinates due to nonlinear effects were carried out during a stage at Politecnico of the third author (GV) within the EC Project ICONS (Contract n. ERBFMRXCT 96002). The second author (RP) acknowledges funding from the National Ministry of Research and Technology (MURST Cofinanziamento 1999, Prot n. 9908262899_004).

REFERENCES

Bellotti R., Jamiolkowski M, Lo Presti D.C.F. and. Neill D.A. [1996]. Anisotropy of Small Strain Stiffness in Ticino Sand, *Geotechnique,* Vol. 46, pp. 115-131.

Budhu, M. and A. Al-Karni [1993]. Seismic bearing capacity of soils. *Géotechnique*, Vol. 43, pp. 181-187.

Butterfield R. and G. Gottardi [1994]. A complete three-dimensional failure envelope for shallow footings on sand. *Géotechnique*, Vol. 44, pp. 181-184.

Cremer C., Pecker A. and L. Davenne [1999]. Elaboration of a soil-structure interaction macro-element with uplift of shallow foundation. Proc. V Colloque National Association Française Génie Parasismique, Cachan, France, pp. 197-206. (In French)

Eurocode 8- Part 5 [1994]. Design Provisions for the Earthquake Resistance of Structures. Part 5: Foundations, Retaining Structures and Geotechnical Aspects. DOC. ENV 1998-5, CEN European Committee for Standardization, Bruxelles, Belgium.

Faccioli E. and R. Paolucci (Eds.) [1996]. *Seismic behaviour and design of foundations and retaining structures*, Technical Report n. 2 ECOEST-PREC8, EC HCM Programme, LNEC Lisbon, Portugal, pp. 212.

Garnier J. and Pecker A. [1999]. Use of Centrifuge Tests for the Validation of Innovative Concepts in Foundation Engineering, *Proc. 2nd Int. Conf. on Earthquake Geotechnical Engineering*, Lisbon, Vol. 1, pp. 433-439.

Gazetas G. [1991]. Foundation vibrations. In *Foundation Engineering Handbook*, 2nd Edition, H.Y. Fang Editor, Van Nostrand Reinhold, New York.

Gazetas [2000]. Overturning and settlement in Adapazari during the Kocaeli 1999 earthquake. *Unpublished memorandum.*

Gottardi G., Houlsby G.T. and R. Butterfield [1999]. Plastic response of circular footings on sand under general planar loading. *Géotechnique*, Vol. 49, pp. 453-469.

Jamiolkowski M., Lo Presti D.C.F., Puci I., Negro P., Verzeletti G., Molina J.F., Faccioli E., Pedretti S., Pedroni S., Morabito P. [1999]. Large Scale Geotechnical Experiments on Soil-Foundation Interaction, *Proc. 2nd Int. Sym. on Pre-Failure Deformation Characteristics of Geomaterials*, Turin.

Lambe T.W and R.V. Whitman [1969]. *Soil Mechanics.* John Wiley and Sons Eds, NY.

Le Pape Y., J.-F. Sieffert and P. Harlicot [1999]. Non linear seismic analysis of shallow footing behaviour using macro-elements. Proc. V Colloque National Association Française Génie Parasismique, Cachan, France, pp. 207-214. (In French)

Negro P., Pinto A.V., Verzeletti G., Magonette G.E. [1996]. PsD Test on a Four-Story R/C Building Designed According to Eurocodes, *Journal of Structural Engineering*, ASCE, Vol. 122, pp. 1409-1417.

Newmark N.M. [1965]. Effects of earthquakes on dams and embankments. *Géotechnique*, Vol. 15, pp. 139-160.

Nova R. and L. Montrasio [1991]. Settlements of shallow foundations on sand. *Géotechnique*, Vol. 41, pp. 243-256.

Paolucci R. [1997]. Simplified evaluation of earthquake induced permanent displacements of shallow foundations. *J. of Earthquake Engineering* , Vol. 1, pp. 563-579.

Paolucci R. and A. Pecker [1997a] Seismic bearing capacity of shallow strip foundations on dry soils. *Soils and Foundations*, Vol. 37, pp. 95-105.

Paolucci R. and A. Pecker [1997b]. Soil inertia effects on the bearing capacity of rectangular foundations on cohesive soils. *Engineering Structures*, Vol. 19, pp. 637-643.

Pecker A. and J. Salençon [1991]. Seismic bearing capacity of shallow strip foundations on clay soils. *Proc. Int. Workshop on Seismology and Earthq. Engng.*, CENAPRED, Mexico City, 287-304.

Pecker, A. [1997] Analytical formulae for the seismic bearing capacity of shallow strip foundations. In *Seismic Behaviour of Ground and Geotechnical Structures*, Ed. Seco e Pinto, Balkema, pp. 261-268.

Pecker A. [1998]. Capacity design principles for shallow foundations in seismic areas. *Proc. XI Europ. Conf. on Earthquake Engineering*, Paris, CD Rom.

Pedretti S. [1998]. Nonlinear soil-foundation interaction: analysis and modelling methods. PhD Thesis in Earthquake Engineering. Politecnico di Milano, Italy.

Richards R., D.G. Elms and M. Budhu [1993]. Seismic bearing capacity and settlements of shallow foundations. *Journ. Geotech. Engng. ASCE*, Vol. 119, pp. 662-674.

Sarma S.K. and I.S. Iossifelis [1990]. Seismic bearing capacity factors of shallow strip footings. *Géotechnique*, Vol. 40, pp. 265-273.

Seed H.B., Wong R.T. and I.M. Idriss [1986]. Soil moduli and damping factors for dynamic analyses of cohesionless soils. *Journ. Geotech. Engng. ASCE*, Vol. 112, pp. 1016-1032.

Taylor C.A., Dar A.R. and Crewe A.J. [1994]. Shaking Table Modelling of Seismic Geotechnical Problems. *Proc. 10th Europ. Conf. on Earthq. Engineering*, Vienna, Vol. 1, pp. 441-446.

Vesic A. [1973]. Analysis of ultimate loads of shallow foundations. *Journ. Geotech. Engng. ASCE*, Vol. 99, pp. 45-73.

Vivero G. [2000]. Effects of soil plasticity on railway bridges. Technical report, Politecnico di Milano, EC Contract n. ERB FMRX CT96 0022, TMR Programme.

Zeng X. and R.S. Steedman [1998]. Bearing capacity failure of shallow foundations in earthquakes. *Géotechnique*, Vol. 48, pp. 235-256.